



# HHS Public Access

Author manuscript

*Chem Res Toxicol.* Author manuscript; available in PMC 2017 February 05.

Published in final edited form as:

*Chem Res Toxicol.* 2016 December 19; 29(12): 1903–1911. doi:10.1021/acs.chemrestox.6b00136.

## Combining Chimeric Mice with Humanized Liver, Mass Spectrometry, And Physiologically-Based Pharmacokinetic Modeling in Toxicology

Hiroshi Yamazaki<sup>†,\*</sup>, Hiroshi Suemizu<sup>‡</sup>, Marina Mitsui<sup>†</sup>, Makiko Shimizu<sup>†</sup>, and F. Peter Guengerich<sup>§</sup>

<sup>†</sup>Showa Pharmaceutical University, Machida, Tokyo 194-8543, Japan

<sup>‡</sup>Central Institute for Experimental Animals, Kawasaki-ku, Kawasaki 210-0821, Japan

<sup>§</sup>Department of Biochemistry, Vanderbilt University School of Medicine, Nashville, Tennessee 37232-0146

### Abstract

Species differences exist in terms of drug oxidation activities, which are mediated mainly by cytochrome P450 (P450) enzymes. To overcome the problem of species extrapolation, transchromosomal mice containing a human P450 3A cluster or chimeric mice transplanted with human hepatocytes have been introduced into the human toxicology research area. In this review, drug metabolism and disposition mediated by humanized livers in chimeric mice are summarized in terms of biliary/urinary excretions of phthalate and bisphenol A and plasma clearances of the human cocktail probe drugs caffeine, warfarin, omeprazole, metoprolol, and midazolam. Simulation of human plasma concentrations of the teratogen thalidomide and its human metabolites is possible with a simplified physiologically-based pharmacokinetic model based on data obtained in chimeric mice, in accordance with reported clinical thalidomide concentrations. In addition, *in vivo* non-specific hepatic protein binding parameters of metabolically activated <sup>14</sup>C-drug candidate and hepatotoxic medicines in humanized liver mice can be analyzed by accelerator mass spectrometry and are useful for predictions in humans.

### Graphical Abstract

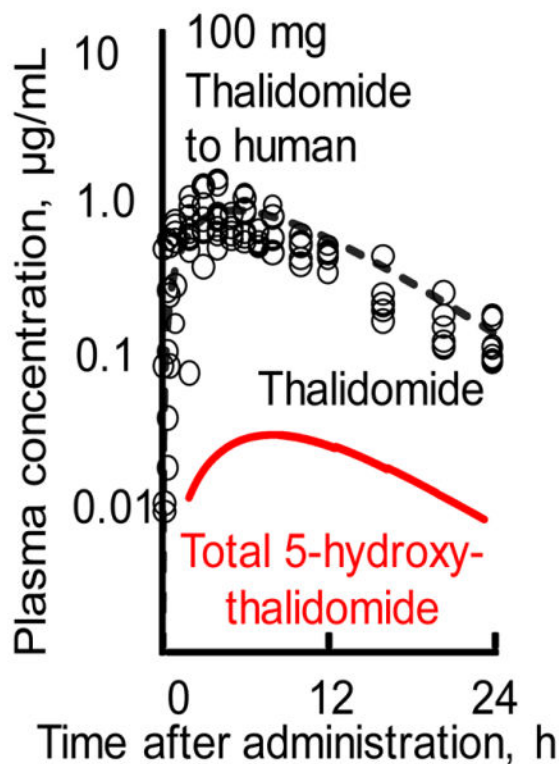
\*Correspondence to: Showa Pharmaceutical University, 3-3165 Higashi-tamagawa Gakuen, Machida, Tokyo 194-8543, Japan. Telephone: +81-42-721-1406; FAX: +81-42-721-1406. hyamazak@ac.shoyaku.ac.jp.

<sup>†</sup>Showa Pharmaceutical University

<sup>‡</sup>Central Institute for Experimental Animals

<sup>§</sup>Vanderbilt University School of Medicine

Description of the Supporting Information material. Table S1 (Parameters for simplified PBPK models for caffeine, warfarin, omeprazole, metoprolol, and midazolam.). This material is available free of charge via the Internet at <http://pubs.acs.org>.



Taken from Chem. Res. Toxicol.  
2015, 28, 2088–2090

## 1. Introduction

The human cytochrome *P450* gene superfamily comprises 57 genes and 58 pseudogenes.<sup>1</sup> The corresponding P450 (P450 or CYP) enzymes are involved in the oxidative metabolism of a variety of endogenous compounds, medicines, and toxic chemicals. Rodents are often used as animal models in drug development, but it is well known that species differences exist in terms of drug metabolism mediated mainly by rodent and human P450s.<sup>2</sup> The relevance and limitations of animal models used in non-clinical safety assessments of investigational products and new medicines needs to be carefully considered. To overcome the species differences, humanized mice have been widely developed by introducing human specific and/or multiple genes for drug metabolizing P450s,<sup>3,4</sup> NAD(P)H:quinone oxidoreductase<sup>5</sup>, and nuclear receptors that control their expression.<sup>6,7</sup> Another type of humanized model mice has been also developed by transplanting human hepatocytes in immunodeficient mice.<sup>8–10</sup> NOG mice expressing transgenic urokinase-type plasminogen activator in the liver were produced,<sup>9</sup> and replacement by human hepatocytes could be estimated by human albumin concentrations in the blood because the humanized mice produces human albumin. Humanized (TK-NOG) mice expressing a herpes simplex virus type 1 thymidine kinase transgene had a human-specific profile of drug metabolism.<sup>10</sup>

One of the classical species differences is seen in thalidomide, a teratogen in humans or non-human primates<sup>11</sup> but not in rodents. Recently, a whole-embryo culture system from transchromosomal mice containing a human cytochrome P450 3A cluster<sup>12</sup> (in which the endogenous mouse *P450 3a* genes were deleted) showed limb abnormalities,<sup>13</sup> suggesting that the humanized P450 3A mouse is a useful model for predicting toxicity in humans. Thalidomide is metabolized via two major pathways, 5'-hydroxythalidomide (a major product in rodents) and 5-hydroxythalidomide (human proportionate phenyl ring-based metabolites, Figure 1).<sup>14</sup> Furthermore, thalidomide and primary 5-hydroxylated metabolites (including 5,6-dihydroxythalidomide and GSH conjugate(s)) were detected by mass spectrometry (MS) in plasma from chimeric mice with highly "humanized" liver cells harboring cytochrome *P450 3A5\*1*.<sup>14</sup> Chimeric mice with humanized liver revealed that the second oxidation step in human proportionate 5-hydroxythalidomide pathway generated a reactive intermediate that can be trapped by GSH to give GSH adducts,<sup>14</sup> indicating that this model is useful for predicting toxic metabolites in humans.

*In vitro-in vivo* extrapolations of hepatic clearance and disposition have been reported for a wide variety of drugs.<sup>15</sup> Simplified physiologically-based pharmacokinetic (PBPK) models consist of a chemical receptor compartment, a metabolizing compartment, and a central compartment (Figure 2).<sup>14,16,17</sup> Subsequently, final parameter values (including standard deviation values) for an animal PBPK model can be calculated to give the best fit to measured blood substrate concentration values. Differential equations can be solved to estimate blood concentrations of substrates and/or metabolites after oral administration.<sup>14,16,17</sup> These simplified human PBPK models for industrial chemicals with toxicity concerns (e.g., bisphenol A<sup>17</sup> and di(2-ethylhexyl)phthalate<sup>16</sup> and the pesticides acephate<sup>18</sup> and chlorpyrifos<sup>18</sup>) were recently developed and successfully used to estimate human pharmacokinetic parameters, based on the pharmacokinetics in humanized mice.

There is considerable interest in the importance of drug metabolites as potential determinants of drug safety.<sup>19</sup> Guidance notes for Industry Safety Testing of Drug Metabolites (issued in 2008 by the United States Food and Drug Administration) laid out criteria regarding the circumstances under which direct testing of a metabolite in animal toxicology studies is needed to provide a reliable risk assessment of human health. Recent developments in chimeric mice with humanized liver<sup>20</sup> and in bioanalytical methodology with LC-MS/MS systems have provided several strategies to generate data that can guide critical decisions related to metabolite quantitation and biomonitoring in plasma.

In this review article, drug metabolism and disposition mediated by humanized livers in chimeric mice are summarized. These models may be useful for evaluating the relationships between biliary and urinary excretion, clearances in plasma, human metabolite formation, and non-specific protein binding of drugs and their metabolites and the potential toxicity in humans. These findings provide examples of the usefulness of transplanted human liver cells in humanized mice to provide accurate preclinical predictions of human drug metabolism and disposition, with the aid of LC-MS/MS systems.

## 2. Disposition and Clearance of Industrial Chemicals and Human P450 Probe Drugs in Humanized Liver Mice

Species variations in the threshold molecular weight factor for the biliary excretion of orally administered compounds have been recognized in mice ( $325 \pm 50$ ) and humans ( $500 \pm 50$ );<sup>21</sup> urinary excretion is extensive for the compounds of lower molecular weight and tends to decrease with increasing molecular weight because bile and urine are complementary excretory pathways in animals. Although a renal clearance-type drug (cefmetazole) has been mainly excreted in urines of humanized mice urine but not in control mice,<sup>22</sup> the hepatic metabolite excretion into urine was not confirmed in humanized mice.

In immunodeficient TK-NOG mice, transplanted human hepatocytes (which express similar human P450 mRNA levels and have catalytic function as transplanted human hepatocytes) were maintained after an initial exposure to a non-toxic dose of ganciclovir to ablate the mouse liver cells.<sup>10</sup> The pharmacokinetics of mono(2-ethylhexyl)phthalate (MEHP) (a primary metabolite of di(2-ethylhexyl)phthalate (DEHP))<sup>16</sup> and bisphenol A *O*-glucuronide<sup>17</sup> (after oral administration of DEHP (250 mg/kg) and bisphenol A (100 mg/kg)) were determined in order to extrapolate these experimental data from chimeric mice transplanted with human hepatocytes to virtual administration in humans. Biphasic plasma concentration–time curves of MEHP and its glucuronide and high fecal excretion levels of MEHP glucuronide were seen in control mice, although MEHP and its glucuronide were extensively excreted in urine within 24 h in mice when humanized liver mice were used.

For running simple PBPK modeling, physicochemical properties (i.e. plasma unbound fraction and octanol–water partition coefficients) and the pharmacokinetic parameters (e.g., absorption rate constant ( $k_a$ ), volume of the systemic circulation ( $V_1$ ), and hepatic intrinsic clearance ( $CL_{h,int}$ )) were estimated and calculated by fitting.<sup>16,17</sup> Typical physiological hepatic blood flow rates in mice (0.16 L/h) and humans (97 L/h) were used.<sup>23,24</sup> Using known species allometric scaling factors, estimated urine MEHP concentrations in humans based on the pharmacokinetics in mice with humanized liver by a simple PBPK model<sup>16</sup> were consistent with the reported concentrations.<sup>25</sup> These findings showed that transplanted human hepatocytes could affect the extensive excretion of primary and secondary metabolites of DEHP into urine in chimeric mice, as in the cases of marmosets<sup>26</sup> or humans.<sup>25</sup> Simplified PBPK models were used with both forward and reverse dosimetry and were able to estimate human plasma and urinary concentrations of MEHP<sup>16</sup> and bisphenol A *O*-glucuronide after ingestion of bisphenol A<sup>17</sup>. The Fourth National Report on Human Exposure to Environmental Chemicals, Updated Tables, August 2014 (U. S. Centers for Disease Control)<sup>27</sup> indicates geometric means and 95th percentile values of urinary MEHP concentrations for men in the USA in 2005–2006 of 3.4 and 50  $\mu\text{g/L}$ , respectively. Urinary total concentrations of bisphenol A in the US population in 2003–2004 were 2.6 and 16  $\mu\text{g/L}$ , respectively, which were the highest values recorded in the period 1999–2010. The MEHP concentrations in urine can be ascribed to exposure of 0.087  $\mu\text{g/kg/day}$  and 1.3  $\mu\text{g/kg/day}$  DEHP and to 0.067  $\mu\text{g/kg/day}$  and 0.41  $\mu\text{g/kg/day}$  bisphenol A, respectively, by reverse dosimetry with the human PBPK model (Table 1), assuming that the reported urinary concentrations had reached steady-state values. These estimated DEHP and bisphenol A

exposures are far less than the daily tolerable intake of DEHP (30  $\mu\text{g}/\text{kg}/\text{day}$ <sup>28,29</sup> or 50  $\mu\text{g}/\text{kg}/\text{day}$ , EU Public Health, 2008) and daily tolerable intake of bisphenol A (50  $\mu\text{g}/\text{kg}/\text{day}$ ),<sup>30</sup> implying little risk of either compound in humans under average conditions.

This simple system was also successful in estimating human plasma concentrations of various P450 probes based on non-human primate, dog, and minipig plasma data<sup>31–33</sup>. This simple system was also successful in estimating human plasma concentrations of various P450 probes in humans extrapolated from corresponding plasma data in humanized liver mice and marmosets,<sup>32</sup> dogs<sup>31</sup>, minipigs<sup>31</sup>, and monkeys.<sup>33</sup> Pharmacokinetic parameters for humanized liver mice and other animals (marmosets, monkeys, dogs, and minipigs) determined in *in vivo* experiments with P450 cocktail probes using LC-MS/MS methods described elsewhere.<sup>31–33</sup> are described (Table 2). Briefly, observed plasma concentrations of caffeine, warfarin, omeprazole, metoprolol, and midazolam in chimeric TK-NOG mice with humanized liver were scaled to human oral monitoring equivalents using known species allometric scaling factors. Human plasma concentration profiles of the five P450 probes estimated by simplified human PBPK models (based on the observed pharmacokinetics in mice with humanized liver) were consistent with previously published pharmacokinetic data in Caucasians (Figure 3). Similarly, using the same approach, the previously reported pharmacokinetics of the five P450 probes in marmosets, monkeys, dogs, and minipigs (Supporting Table S1) were also scaled to reported equivalents in humans using *in vitro* metabolic clearance data.<sup>31,33</sup> The results in Figure 3 (created with the parameters in Supporting Table S1) suggest that mice with humanized liver and/or marmosets, monkeys, dogs, and minipigs can be used as suitable pharmacokinetic models for humans during research with many new drugs, especially when used in combination with simple PBPK models with LC-MS/MS analytical systems for drug monitoring. Human hepatic clearance values of omeprazole, metoprolol, and midazolam in the simple PBPK models based on humanized mice and average parameters for humans were 52.2 and 40.9 ( $\pm 9.9$ ) L/h, 46.5 and 55.9 ( $\pm 10.6$ ) L/h, and 31.7 and 41.5 ( $\pm 10.4$ ) L/h, respectively (Table 2). The expected  $\text{AUC}_{\text{last}}$  values on virtual administrations with average parameters for five human models of omeprazole ( $407 \pm 216 \text{ ng h}^{-1} \text{ mL}^{-1}$ ), metoprolol ( $939 \pm 347 \text{ ng h}^{-1} \text{ mL}^{-1}$ ), and midazolam ( $37.5 \pm 17.4 \text{ ng h}^{-1} \text{ mL}^{-1}$ ) were consistent with 30 reported human averages ( $\pm$  SD values) for omeprazole ( $368 \pm 250 \text{ ng h}^{-1} \text{ mL}^{-1}$ ), metoprolol ( $449 \pm 303 \text{ ng h}^{-1} \text{ mL}^{-1}$ ), and midazolam ( $27.3 \pm 8.0 \text{ ng h}^{-1} \text{ mL}^{-1}$ ). Caffeine and *S*-warfarin, having intermediate and low hepatic extraction ratio drugs, respectively, also showed good consistency between estimated and reported AUC values in the present system (Table 2).

### 3. Metabolic Activation of Thalidomide in Humanized Liver Mice

The metabolism of thalidomide is important for both teratogenicity and anti-cancer efficacy. Thalidomide is metabolized via P450-mediated oxidation.<sup>34</sup> Various P450s oxidize thalidomide to 5-hydroxy-, 5'-hydroxy-, and dihydroxythalidomide products (Figure 1A), with a major one being P450 2C19.<sup>35,36</sup> Recently we reported that human P450 3A4 and 3A5 also oxidize thalidomide to the 5-hydroxy and dihydroxy metabolites.<sup>37–39</sup> The second oxidation step in the P450 3A4 pathway generates a reactive intermediate, possibly an arene oxide (as initially suggested by Gordon *et al.*<sup>40</sup> that can be trapped by GSH to give GSH adducts, as confirmed in humanized mouse models using LC-MS/MS methods.<sup>38,39</sup> The

secondary oxidation of 5-hydroxythalidomide was faster than the primary thalidomide 5-hydroxylation mediated by recombinant human P450 3A4/5.<sup>37</sup> Thalidomide and its human metabolite 5-hydroxythalidomide were oxidized by auto-induced human P450 3A enzymes<sup>41</sup> to reactive intermediates (with substrate cooperativity<sup>42</sup>), with reactive sites on the aromatic ring, i.e. epoxides and *o*-quinones that were trapped as glutathione conjugates.<sup>37,39</sup>

The primary metabolite 5-hydroxythalidomide was found to be extensively oxidized by human P450 enzymes to a dihydroxy metabolite.<sup>43</sup> The dihydroxy metabolite is further oxidized to a quinone intermediate that can be trapped with GSH to give a dihydroxythalidomide-GSH conjugate. The observation that quinones are known to undergo redox cycling to generate reactive oxygen species may be consistent with a proposed reactive oxygen species hypothesis for toxicity.<sup>44</sup> Based on the *in vivo* experiments in humanized liver mice<sup>45</sup> (Figure 4A), results following administration of a low dose of 100 mg thalidomide to human subjects could be reasonably estimated by the current simplified human PBPK model (Figure 4A).<sup>14</sup>

#### 4. Metabolic Activation of Hepatotoxicant and Non-Specific Binding in Humanized Liver Mice

Drug-induced liver injury is one of the most frequent single causes of safety-related withdrawals of drugs from the market.<sup>46</sup> The National Institutes of Health LiverTox database (<http://livertox.nih.gov/>) is a free online source of textual documents on liver injury caused by prescription and nonprescription drugs, collected from various databases.<sup>47</sup> Recently, systematic research into metabolic drug activation has become more comprehensive and more complex.<sup>48</sup> Drug-induced toxicity may be caused by active intermediates, formed especially by human cytochrome P450 enzymes. In a clinical study of 5-*n*-butyl-7-(3,4,5-trimethoxybenzoylamino)pyrazolo[1,5-*a*]pyrimidine (OT-7100, an amide moiety-bearing pyrazolopyrimidine derivative with potential analgesic effects),<sup>49</sup> limited elevations in the serum levels of aspartate or alanine aminotransferase were occasionally observed in humans; these elevations were not predicted from regulatory animal or *in vitro* studies.<sup>50</sup> As an example of species differences in metabolic drug activation, human liver P450 1A2 differed from rat P450 1A2 in bioactivation of the primary metabolite of 5-*n*-butyl-7-(3,4,5-trimethoxybenzoylamino)pyrazolo[1,5-*a*]pyrimidine (an amide moiety-bearing pyrazolopyrimidine derivative with potential analgesic effects).<sup>50</sup> A primary metabolite was oxidized by human P450 1A2 to form a proximate metabolite, which was conjugated with a peptide to form an adduct (Figure 1B).<sup>51</sup> In rats, the same P450 1A2 enzyme formed some proximate metabolites but predominantly mediated the formation of another metabolite that exhibited no toxicity.<sup>52</sup> These metabolic differences highlight some of the perils of relying solely on animal testing of drug candidates for metabolite toxicity.

Electrophoretic zone analysis coupled with accelerator MS methods revealed that bioactivated radiolabeled diazepam (rarely hepatotoxic) and 5-*n*-butyl-pyrazolo[1,5-*a*]pyrimidine (Figure 5, limited hepatotoxicity) bound nonspecifically *in vivo* to a variety of microsomal and/or cytosolic proteins present in liver from chimeric mice with humanized

liver.<sup>53</sup> A line is drawn through convenient axis intersections to indicate an inverse relationship (Figure 5). In contrast, radiolabeled troglitazone and flutamide (both known to be hepatotoxic in humans) showed relatively little covalent binding at concentrations needed for target protein binding.<sup>53</sup> These two idiosyncratic hepatotoxic drugs were activated to reactive metabolites and apparently bound to different target proteins. Thus, testing whether protein binding data of new drug candidates are unbalanced with respect to deviation from an inverse relationship like the case in Figure 5 or the presence of data points in the high covalent binding/high protein concentration zone can be an important concept in evaluating hepatotoxic potential.<sup>53</sup> To understand the roles of human P450 enzymes in drug metabolism, safety assessment of drug metabolites in engineered mouse models is proposed for more extensive use.

## 5. Conclusions and future perspective

Current research collectively suggests that studies of drug metabolism using transplanted human liver cells in humanized mice may be useful in evaluating the drug clearance and disposition, human metabolite formation, and non-specific protein binding tendency of drugs and their metabolites and potential toxicity in humans. Recently, transplantation of three-dimensional-cultured hepatoma-derived cell line HepaRG cells has been reported to yield hepatocyte-like colonies in *in vivo* mouse bodies, like primary human hepatocytes, suggesting a possible human cell source for steady generation of humanized liver TK-NOG mice.<sup>54,55</sup> Humanized mice reconstituted with human immune systems are also essential to study human immune reactions *in vivo* and are expected to be useful for studying human allergies. A novel transgenic NOG strain bearing human *interleukin-3* and *granulocyte macrophage colony-stimulating factor* genes has been developed.<sup>56</sup> Combinations of transplanted human hepatocytes and immune system may become available in the future to study human-type drug metabolite identification and resulting human immune reactions in the combined model of humanized mice. These humanized model mice provide accurate preclinical predictions of human drug metabolism and disposition, coupled with MS methods.

## Supplementary Material

Refer to Web version on PubMed Central for supplementary material.

## Acknowledgments

The authors thank Prof. Norio Shibata and Drs. Koichiro Adachi, Takamori Miyaguchi, Sayako Nishiyama, Satomi Shida, Mirai Kawano, Shotaro Uehara, and Norie Murayama for their experimental support.

**Funding Sources.** This work was supported in part by the Japan Society for the Promotion of Science Grants-in-Aid for Scientific Research 26460206 (H.Y.), the MEXT (Ministry of Education, Science, Sports and Culture of Japan)-Supported Program for the Strategic Research Foundation at Private Universities, 2013–2018. and United States Public Health Service grant R01 GM118122 (F.P.G.).

## Abbreviations

MS            mass spectrometry

**NOG mice** non-obese diabetes-severe combined immunodeficiency-interleukin-2 receptor gamma chain-deficient mice

## References

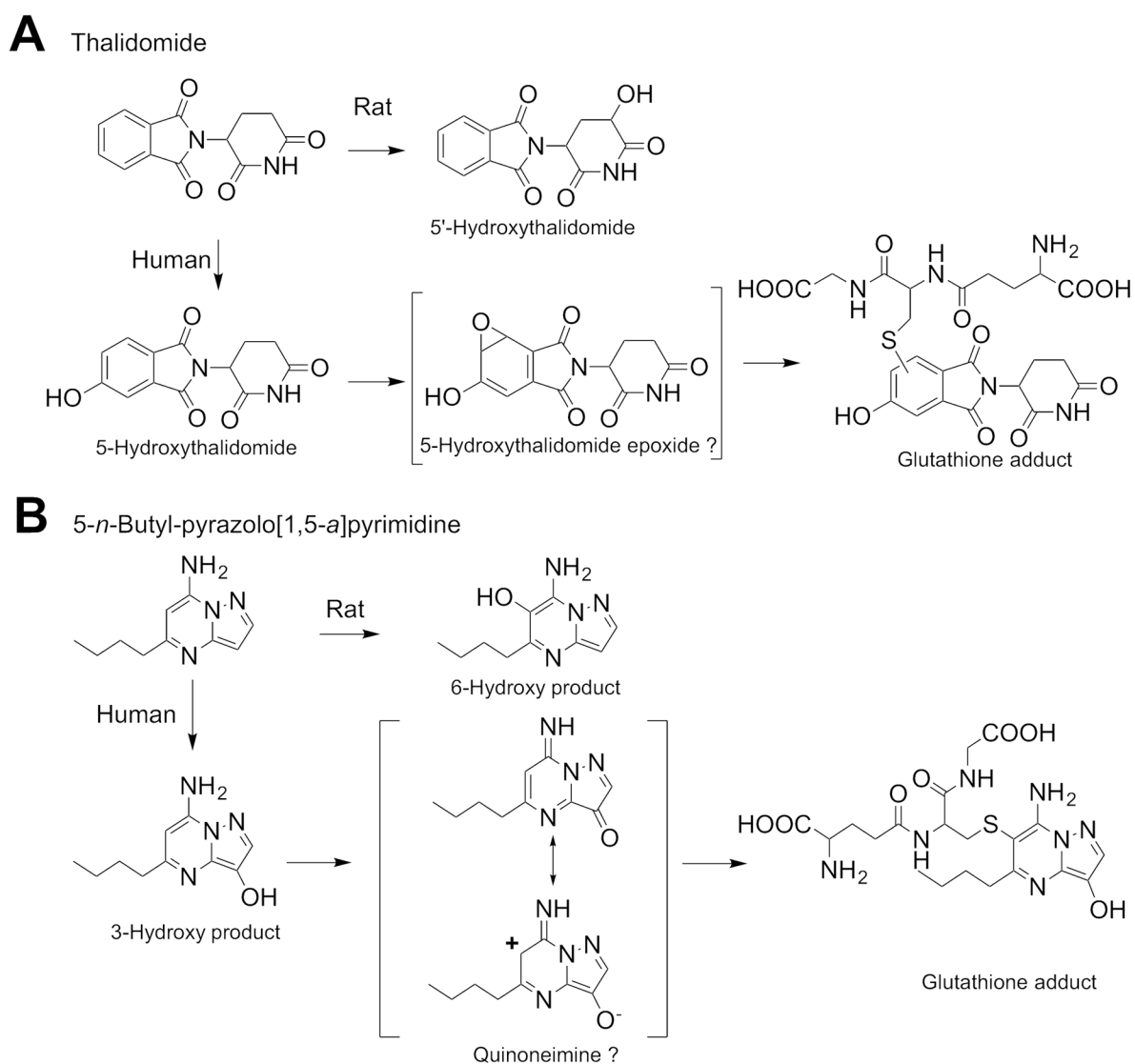
1. Nelson DR, Zeldin DC, Hoffman SMG, Maltais LJ, Wain HM, Nebert DW. Comparison of cytochrome P450 (*CYP*) genes from the mouse and human genomes, including nomenclature recommendations for genes, pseudogenes and alternative-splice variants. *Pharmacogenetics*. 2004; 14:1–18. [PubMed: 15128046]
2. Guengerich FP. Cytochrome P450 and chemical toxicology. *Chem Res Toxicol*. 2008; 21:70–83. [PubMed: 18052394]
3. Gonzalez FJ, Fang ZZ, Ma X. Transgenic mice and metabolomics for study of hepatic xenobiotic metabolism and toxicity. *Expert Opin Drug Metab Toxicol*. 2015; 11:869–881. [PubMed: 25836352]
4. Scheer N, Kapelyukh Y, Rode A, Oswald S, Busch D, McLaughlin LA, Lin D, Henderson CJ, Wolf CR. Defining human pathways of drug metabolism in vivo through the development of a multiple humanized mouse model. *Drug Metab Dispos*. 2015; 43:1679–1690. [PubMed: 26265742]
5. Levova K, Moserova M, Nebert DW, Phillips DH, Frei E, Schmeiser HH, Arlt VM, Stiborova M. NAD(P)H:quinone oxidoreductase expression in *Cyp1a*-knockout and *CYP1A*-humanized mouse lines and its effect on bioactivation of the carcinogen aristolochic acid I. *Toxicol Appl Pharmacol*. 2012; 265:360–367. [PubMed: 22982977]
6. Moriguchi T, Motohashi H, Hosoya T, Nakajima O, Takahashi S, Ohsako S, Aoki Y, Nishimura N, Tohyama C, Fujii-Kuriyama Y, Yamamoto M. Distinct response to dioxin in an arylhydrocarbon receptor (AHR)-humanized mouse. *Proc Natl Acad Sci U S A*. 2003; 100:5652–5657. [PubMed: 12730383]
7. Ma X, Shah Y, Cheung C, Guo GL, Feigenbaum L, Krausz KW, Idle JR, Gonzalez FJ. The PREgnane X receptor gene-humanized mouse: a model for investigating drug-drug interactions mediated by cytochromes P450 3A. *Drug Metab Dispos*. 2007; 3:194–200.
8. Tateno C, Yoshizane Y, Saito N, Kataoka M, Utoh R, Yamasaki C, Tachibana A, Soeno Y, Asahina K, Hino H, Asahara T, Yokoi T, Furukawa T, Yoshizato K. Near completely humanized liver in mice shows human-type metabolic responses to drugs. *Am J Pathol*. 2004; 165:901–912. [PubMed: 15331414]
9. Suemizu H, Hasegawa M, Kawai K, Taniguchi K, Monnai M, Wakui M, Suematsu M, Ito M, Peltz G, Nakamura M. Establishment of a humanized model of liver using NOD/Shi-scid IL2Rgnull mice. *Biochem Biophys Res Commun*. 2008; 377:248–252. [PubMed: 18840406]
10. Hasegawa M, Kawai K, Mitsui T, Taniguchi K, Monnai M, Wakui M, Ito M, Suematsu M, Peltz G, Nakamura M, Suemizu H. The reconstituted ‘humanized liver’ in TK-NOG mice is mature and functional. *Biochem Biophys Res Commun*. 2011; 405:405–410. [PubMed: 21238430]
11. Poswillo DE, Hamilton WJ, Sopher D. The marmoset as an animal model for teratological research. *Nature*. 1972; 239:460–462. [PubMed: 4628135]
12. Kazuki Y, Kobayashi K, Aueviriyavit S, Oshima T, Kuroiwa Y, Tsukazaki Y, Senda N, Kawakami H, Ohtsuki S, Abe S, Takiguchi M, Hoshiya H, Kajitani N, Takehara S, Kubo K, Terasaki T, Chiba K, Tomizuka K, Oshimura M. Trans-chromosomal mice containing a human CYP3A cluster for prediction of xenobiotic metabolism in humans. *Hum Mol Genet*. 2013; 22:578–592. [PubMed: 23125282]
13. Kazuki Y, Akita M, Kobayashi K, Osaki M, Satoh D, Abe S, Takehara S, Kazuki K, Yamazaki H, Kamataki T, Oshimura M. Thalidomide-induced limb abnormalities in a humanized CYP3A mouse model. *Sci Rep*. 2016; 6:21419. [PubMed: 26903378]
14. Nishiyama S, Suemizu H, Shibata N, Guengerich FP, Yamazaki H. Simulation of human plasma concentrations of thalidomide and primary 5-hydroxylated metabolites explored with pharmacokinetic data in humanized TK-NOG mice. *Chem Res Toxicol*. 2015; 28:2088–2090. [PubMed: 26492539]



15. Poulin P, Haddad S. Hepatocyte composition-based model as a mechanistic tool for predicting the cell suspension: aqueous phase partition coefficient of drugs in in vitro metabolic studies. *J Pharm Sci.* 2013; 102(8):2806–2818. [PubMed: 23670739]
16. Adachi K, Suemizu H, Murayama N, Shimizu M, Yamazaki H. Human biofluid concentrations of mono(2-ethylhexyl)phthalate extrapolated from pharmacokinetics in chimeric mice with humanized liver administered with di(2-ethylhexyl)phthalate and physiologically based pharmacokinetic modeling. *Environ Toxicol Pharmacol.* 2015; 39:1067–1073. [PubMed: 25867688]
17. Miyaguchi T, Suemizu H, Shimizu M, Shida S, Nishiyama S, Takano R, Murayama N, Yamazaki H. Human urine and plasma concentrations of bisphenol A extrapolated from pharmacokinetics established in in vivo experiments with chimeric mice with humanized liver and semi-physiological pharmacokinetic modeling. *Regul Toxicol Pharmacol.* 2015; 72:71–76. [PubMed: 25805149]
18. Suemizu H, Sota S, Kuronuma M, Shimizu M, Yamazaki H. Pharmacokinetics and effects on serum cholinesterase activities of organophosphorus pesticides acephate and chlorpyrifos in chimeric mice transplanted with human hepatocytes. *Regul Toxicol Pharmacol.* 2014; 70:468–473. [PubMed: 25158275]
19. Gao H, Jacobs A, White RE, Booth BP, Obach RS. Meeting report: Metabolites in safety testing (MIST) Symposium-Safety assessment of human metabolites: What’s REALLY necessary to ascertain exposure coverage in safety tests? *AAPS J.* 2013; 15:970–973. [PubMed: 23821354]
20. Kitamura S, Sugihara K. Current status of prediction of drug disposition and toxicity in humans using chimeric mice with humanized liver. *Xenobiotica.* 2014; 44:123–134. [PubMed: 24329499]
21. Hiron PC, Millburn P, Smith RL, Williams RT. Species variations in the threshold molecular-weight factor for the biliary excretion of organic anions. *Biochem J.* 1972; 129:1071–1077. [PubMed: 4656593]
22. Okumura H, Katoh M, Sawada T, Nakajima M, Soeno Y, Yabuuchi H, Ikeda T, Tateno C, Yoshizato K, Yokoi T. Humanization of excretory pathway in chimeric mice with humanized liver. *Toxicol Sci.* 2007; 97:533–538. [PubMed: 17341479]
23. Kato M, Shitara Y, Sato H, Yoshisue K, Hirano M, Ikeda T, Sugiyama Y. The quantitative prediction of CYP-mediated drug interaction by physiologically based pharmacokinetic modeling. *Pharm Res.* 2008; 25:1891–1901. [PubMed: 18483837]
24. Gargas ML, Andersen ME, Teo SKO, Batra R, Fennell TR, Kedderis GL. A physiologically based dosimetry description of acrylonitrile and cyanoethylene oxide in the rat. *Toxicol Appl Pharmacol.* 1995; 134:185–194. [PubMed: 7570594]
25. Kurata Y, Shimamura N, Katoh M. Metabolite profiling and identification in human urine after single oral administration of DEHP. *J Toxicol Sci.* 2012; 37:401–414. [PubMed: 22467031]
26. Kurata Y, Makinodan F, Shimamura N, Katoh M. Metabolism of di (2-ethylhexyl) phthalate (DEHP): comparative study in juvenile and fetal marmosets and rats. *J Toxicol Sci.* 2012; 37:33–49. [PubMed: 22293410]
27. Silva MJ, Barr DB, Reidy JA, Malek NA, Hodge CC, Caudill SP, Brock JW, Needham LL, Calafat AM. Urinary levels of seven phthalate metabolites in the U.S. population from the National Health and Nutrition Examination Survey (NHANES) 1999–2000. *Environ Health Persp.* 2004; 112:331–338.
28. Koch HM, Preuss R, Angerer J. Di(2-ethylhexyl)phthalate (DEHP): human metabolism and internal exposure--an update and latest results. *Int J Androl.* 2006; 29:155–165. [PubMed: 16466535]
29. Rusyn I, Corton JC. Mechanistic considerations for human relevance of cancer hazard of di(2-ethylhexyl) phthalate. *Mutat Res.* 2012; 750:141–158. [PubMed: 22198209]
30. Krishnan K, Gagne M, Nong A, Aylward LL, Hays SM. Biomonitoring equivalents for bisphenol A (BPA). *Regul Toxicol Pharmacol.* 2010; 58:18–24. [PubMed: 20541576]
31. Shida S, Yamazaki H. Human plasma concentrations of five cytochrome P450 probes extrapolated from pharmacokinetics in dogs and minipigs using physiologically based pharmacokinetic modeling. *Xenobiotica.* 2016; 46:759–764. [PubMed: 26652678]

32. Utoh M, Suemizu H, Mitsui M, Kawao M, Toda A, Uehara S, Uno Y, Shimizu M, Sasaki E, Yamazaki H. Human plasma concentrations of cytochrome P450 probe cocktails extrapolated from pharmacokinetics in mice transplanted with human hepatocytes and from pharmacokinetics in common marmosets using physiologically based pharmacokinetic modeling. *Xenobiotica*. in press.
33. Shida S, Utoh M, Murayama N, Shimizu M, Uno Y, Yamazaki H. Human plasma concentrations of cytochrome P450 probes extrapolated from pharmacokinetics in cynomolgus monkeys using physiologically based pharmacokinetic modeling. *Xenobiotica*. 2015; 45:881–886. [PubMed: 26075833]
34. Nakamura K, Matsuzawa N, Ohmori S, Ando Y, Yamazaki H, Matsunaga T. Clinical evidence of the pharmacokinetics change in thalidomide therapy. *Drug Metab Pharmacokinet*. 2013; 28:38–43. [PubMed: 23165864]
35. Ando Y, Fuse E, Figg WD. Thalidomide metabolism by the CYP2C subfamily. *Clin Cancer Res*. 2002; 8:1964–1973. [PubMed: 12060642]
36. Lu J, Helsby N, Palmer BD, Tingle M, Baguley BC, Kestell P, Ching LM. Metabolism of thalidomide in liver microsomes of mice, rabbits, and humans. *J Pharmacol Exp Ther*. 2004; 310:571–577. [PubMed: 15075384]
37. Chowdhury G, Murayama N, Okada Y, Uno Y, Shimizu M, Shibata N, Guengerich FP, Yamazaki H. Human liver microsomal cytochrome P450 3A enzymes involved in thalidomide 5-hydroxylation and formation of a glutathione conjugate. *Chem Res Toxicol*. 2010; 23:1018–1024. [PubMed: 20443640]
38. Yamazaki H, Suemizu H, Igaya S, Shimizu M, Shibata M, Nakamura M, Chowdhury G, Guengerich FP. *In vivo* formation of a glutathione conjugate derived from thalidomide in humanized uPA-NOG mice. *Chem Res Toxicol*. 2011; 24:287–289. [PubMed: 21299192]
39. Yamazaki H, Suemizu H, Shimizu M, Igaya S, Shibata N, Nakamura N, Chowdhury G, Guengerich FP. *In vivo* formation of dihydroxylated and glutathione conjugate metabolites derived from thalidomide and 5-hydroxythalidomide in humanized TK-NOG mice. *Chem Res Toxicol*. 2012; 25:274–276. [PubMed: 22268628]
40. Gordon GB, Spielberg SP, Blake DA, Balasubramanian V. Thalidomide teratogenesis: evidence for a toxic arene oxide metabolite. *Proc Natl Acad Sci U S A*. 1981; 78:2545–2548. [PubMed: 6941308]
41. Murayama N, van Beuningen R, Suemizu H, Guguen-Guillouzo C, Shibata N, Yajima K, Utoh M, Shimizu M, Chesne C, Nakamura M, Guengerich FP, Houtman R, Yamazaki H. Thalidomide increases human hepatic cytochrome P450 3A enzymes by direct activation of pregnane X receptor. *Chem Res Toxicol*. 2014; 27:304–308. [PubMed: 24460184]
42. Yamazaki H, Suemizu H, Murayama N, Utoh M, Shibata N, Nakamura M, Guengerich FP. *In vivo* drug interactions of the teratogen thalidomide with midazolam: Heterotropic cooperativity of human cytochrome P450 in humanized TK-NOG mice. *Chem Res Toxicol*. 2013; 26:486–489. [PubMed: 23419139]
43. Chowdhury G, Shibata N, Yamazaki H, Guengerich FP. Human cytochrome P450 oxidation of 5-hydroxythalidomide and pomalidomide, an amino analog of thalidomide. *Chem Res Toxicol*. 2014; 27:147–156. [PubMed: 24350712]
44. Parman T, Wiley MJ, Wells PG. Free radical-mediated oxidative DNA damage in the mechanism of thalidomide teratogenicity. *Nat Med*. 1999; 5:582–585. [PubMed: 10229238]
45. Nishiyama S, Suemizu H, Shibata N, Guengerich FP, Yamazaki H. Simulation of human plasma concentrations of thalidomide and primary 5-hydroxylated metabolites explored with pharmacokinetic data in humanized TK-NOG mice. *Chem Res Toxicol*. 2015; 28:2088–2090. [PubMed: 26492539]
46. Kaplowitz N. Idiosyncratic drug hepatotoxicity. *Nat Rev Drug Discov*. 2005; 4:489–499. [PubMed: 15931258]
47. Hoofnagle JH, Serrano J, Knoblen JE, Navarro VJ. LiverTox: a website on drug-induced liver injury. *Hepatology*. 2013; 57:873–874. [PubMed: 23456678]
48. Yamazaki H. Drug-induced liver toxicity studies: research into human metabolites clarifies their role in drug development. *Drug Metab Pharmacokinet*. 2014; 29:111. [PubMed: 24769550]

49. Kuribayashi S, Ueda N, Naito S, Yamazaki H, Kamataki T. Species differences in hydrolase activities toward OT-7100 responsible for different bioavailability in rats, dogs, monkeys and humans. *Xenobiotica*. 2006; 36:301–314. [PubMed: 16684710]
50. Kuribayashi S, Goto K, Naito S, Kamataki T, Yamazaki H. Human cytochrome P450 1A2 involvement in the formation of reactive metabolites from a species-specific hepatotoxic pyrazolopyrimidine derivative, 5-*n*-butyl-7-(3,4,5-trimethoxybenzoylamino)pyrazolo[1,5-*a*]pyrimidine. *Chem Res Toxicol*. 2009; 22:323–331. [PubMed: 19138062]
51. Yamazaki H, Kuribayashi S, Inoue T, Tateno C, Nishikura Y, Oofusa K, Harada D, Naito S, Horie T, Ohta S. Approach for *in vivo* protein binding of 5-*n*-butyl-pyrazolo[1,5-*a*]pyrimidine bioactivated in chimeric mice with humanized liver by two-dimensional electrophoresis with accelerator mass spectrometry. *Chem Res Toxicol*. 2010; 23:152–158. [PubMed: 19928966]
52. Kuribayashi S, Uno Y, Naito S, Yamazaki H. Different metabolites of human hepatotoxic pyrazolopyrimidine derivative 5-*n*-butyl-pyrazolo[1,5-*a*]pyrimidine produced by human, rat, and monkey cytochrome P450 1A2 and liver microsomes. *Basic Clin Pharmacol Toxicol*. 2012; 110:405–408. [PubMed: 22017768]
53. Yamazaki H, Kuribayashi S, Inoue T, Honda T, Tateno C, Oofusa K, Ninomiya S, Ikeda T, Izumi T, Horie T. Zone analysis by two-dimensional electrophoresis with accelerator mass spectrometry of *in vivo* protein bindings of idiosyncratic hepatotoxicants troglitazone and flutamide bioactivated in chimeric mice with humanized liver. *Toxicol Res*. 2015; 4:106–111.
54. Higuchi Y, Kawai K, Kanai T, Yamazaki H, Chesne C, Guguen-Guillouzo C, Suemizu H. Functional polymer-dependent 3D culture accelerates the differentiation of HepaRG cells into mature hepatocytes. *Hepatol Res*. in press.
55. Higuchi Y, Kawai K, Yamazaki H, Nakamura M, Bree F, Guillouzo C, Suemizu H. The human hepatic cell line HepaRG cells, possible cell source for steady generation of humanized liver TK-NOG mice. *Xenobiotica*. 2014; 44:146–153. [PubMed: 24066694]
56. Ito R, Takahashi T, Katano I, Kawai K, Kamisako T, Ogura T, Ida-Tanaka M, Suemizu H, Nunomura S, Ra C, Mori A, Aiso S, Ito M. Establishment of a human allergy model using human IL-3/GM-CSF-transgenic NOG mice. *J Immunol*. 2013; 191:2890–2899. [PubMed: 23956433]
57. Turpault S, Brian W, Van HR, Santoni A, Poitiers F, Donazzolo Y, Boulenc X. Pharmacokinetic assessment of a five-probe cocktail for CYPs 1A2, 2C9, 2C19, 2D6 and 3A. *Br J Clin Pharmacol*. 2009; 68:928–935. [PubMed: 20002088]
58. Eriksson T, Bjorkman S, Roth B, Bjork H, Hoglund P. Hydroxylated metabolites of thalidomide: formation *in-vitro* and *in-vivo* in man. *J Pharm Pharmacol*. 1998; 50:1409–1416. [PubMed: 10052858]

**Figure 1.**

Metabolic pathways of thalidomide (A) and 5-*n*-butyl-pyrazolo[1,5-*a*]pyrimidine (B).

Proposed formation of the glutathione conjugate (A) is modified from Chowdhury et al.<sup>43</sup>.

Proposed mechanism for a putative quinone imine metabolite and conjugate formation at the 6-position (B) is taken from Kuribayashi et al.<sup>50</sup>

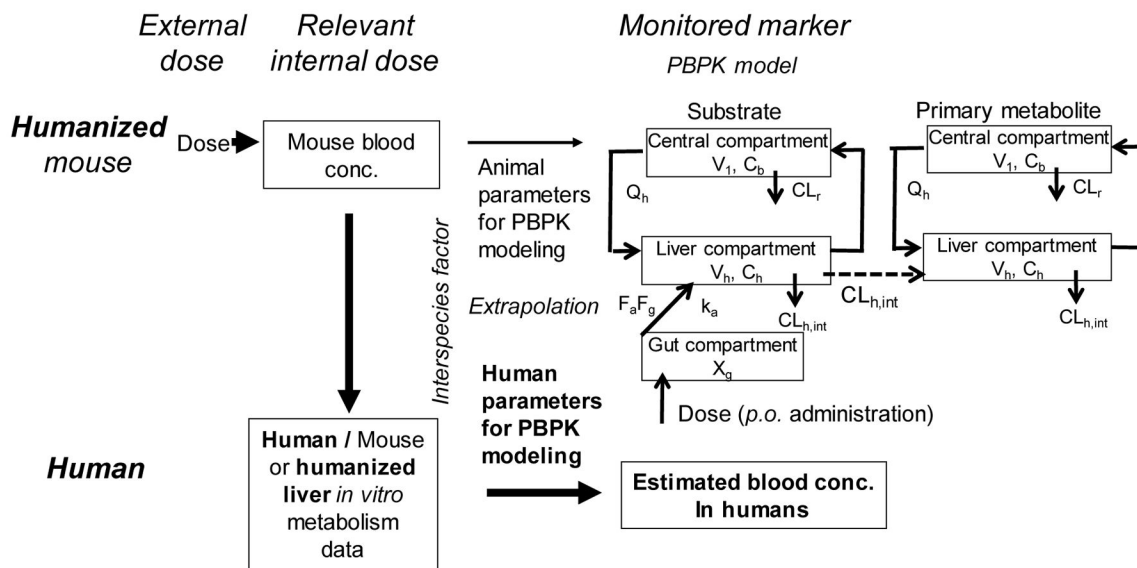


**Figure 2.**  
PBPK model for animals, humanized TK-NOG mice, and humans.

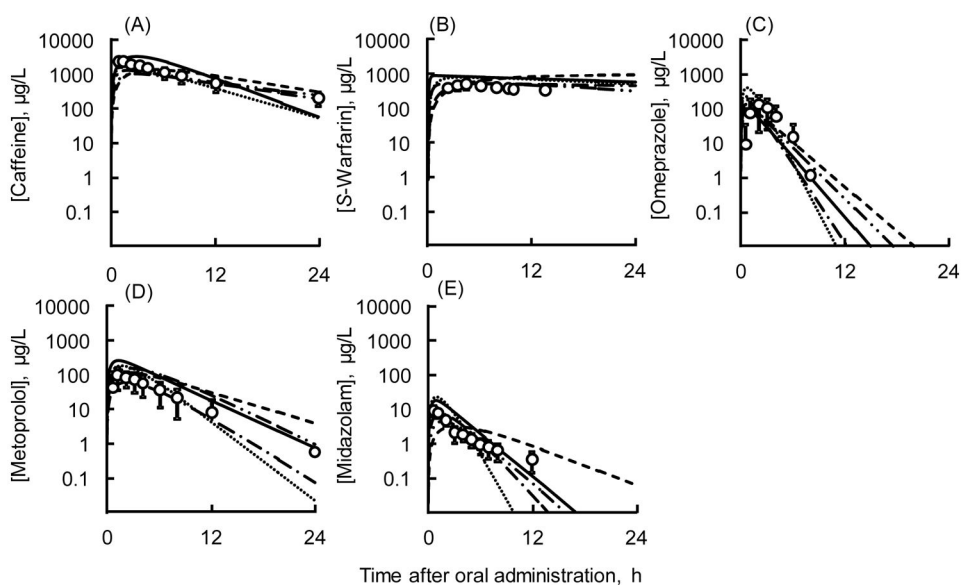


**Figure 3.** Results of simplified human PBPK models for caffeine (A), *S*-warfarin (B), omeprazole (C), metoprolol (D), and midazolam (E) after virtual single oral doses. Solid ( — ) and broken ( ..... ), ( - - - ), ( - · - ), and ( — · · ) lines show simplified human PBPK models based on humanized TK-NOG mouse, marmoset, cynomolgus monkey, dog, and minipig PBPK models, respectively. Circles (with SD bars) show reported mean human plasma concentrations after single oral administration of a combination of five probe drugs to 30 Caucasian subjects (2.1 mg/kg for midazolam, 10 mg for *S*-warfarin, 20 mg for omeprazole, and 100 mg for caffeine and metoprolol).<sup>57</sup>

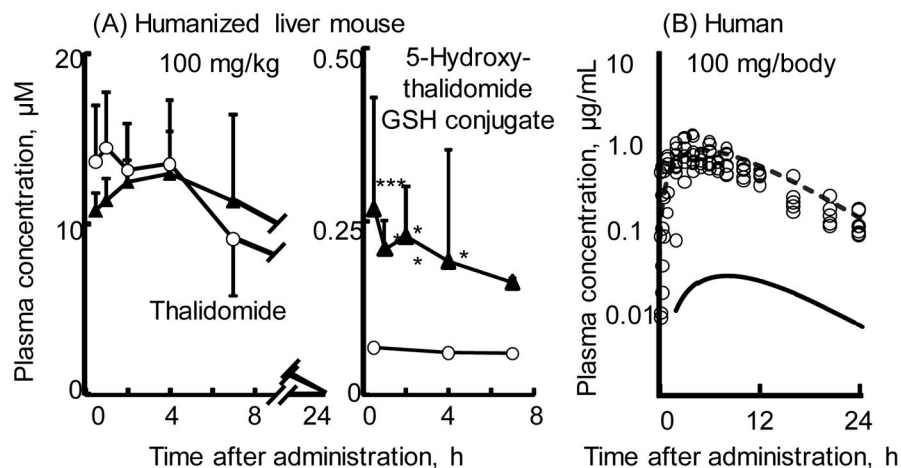


**Figure 4.** Plasma concentrations of thalidomide and 5-hydroxythalidomide-GSH conjugate (A) measured in control TK-NOG mice (open circles) and chimeric TK-NOG mice with humanized liver cells (solid triangles) and thalidomide (open circles, reported by Eriksson *et al.*<sup>58</sup>; broken lines) and the sum of 5-hydroxythalidomide metabolites containing 5-hydroxythalidomide-GSH conjugate and 5,6-dihydroxythalidomide (solid lines) estimated in humans *in silico* after oral administration of a single dose of thalidomide (100 mg/kg for mice and 100 mg for humans). Results are expressed as mean values ( $\pm$  SD) obtained with four mice (\*\* $p < 0.01$ , and \* $p < 0.05$ , two-way ANOVA with Bonferroni post tests). Results are reproduced from Nishiyama *et al.*<sup>14</sup>

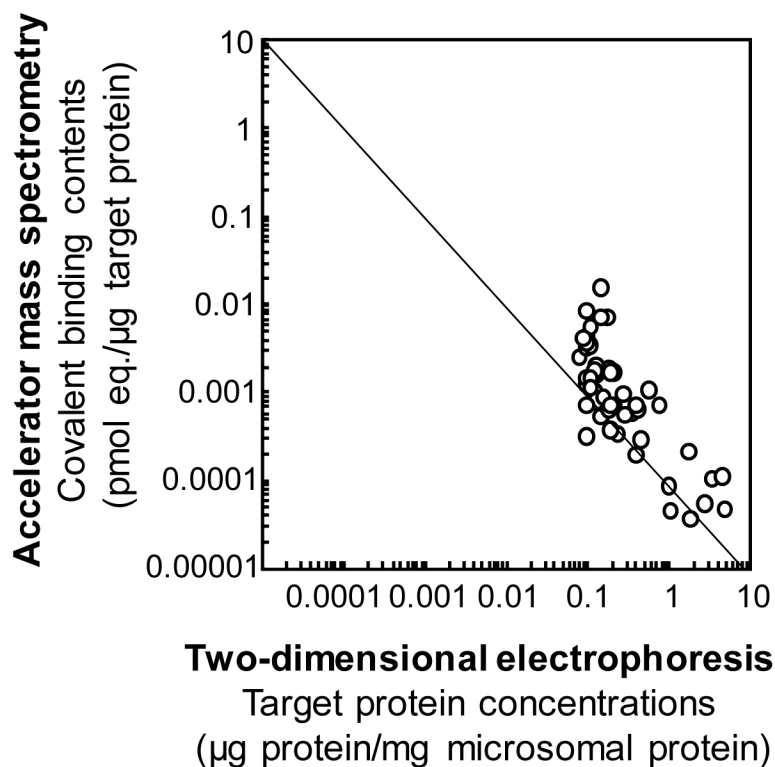


**Figure 5.** Covalent binding profiles of liver microsomal protein fractions separated by two-dimensional electrophoresis. Loaded liver protein samples (100  $\mu\text{g}$ ) were subjected to isoelectric focusing (pI 3–10) and were then separated by sodium dodecyl sulfate-polyacrylamide gel electrophoresis (10–225 kDa). *In vivo* liver protein bindings with metabolically activated  $^{14}\text{C}$ -substrates in humanized liver mice were analyzed by accelerator mass spectrometry. The results for 5-*n*-butyl-pyrazolo[1,5-*a*]pyrimidine, a new drug candidate OT-7100 metabolite, are taken from Yamazaki *et al.*<sup>51</sup>



**Table 1**

Reported urinary concentrations of DEHP and bisphenol A and their estimated exposures.

	urinary concentrations for men in USA, $\mu\text{g/L}$	estimated exposure, $\mu\text{g/kg/day}$	daily tolerated intake, $\mu\text{g/kg/day}$	
D(M)EHP (2005–2006)	geometric mean, 95th percentile,	3.4	0.087	30 or 50
		50	1.3	
bisphenol A (2003–2004)	geometric mean, 95th percentile,	2.6	0.067	50
		16	0.41	

Details are presented in the text.

Author Manuscript

Author Manuscript

Author Manuscript

Author Manuscript

Table 2

Mean parameters for simplified human PBPK models for caffeine, warfarin, omeprazole, metoprolol, and midazolam calculated from parameters in humanized mice, marmosets, cynomolgus monkey, dog, and minipig models.

probe drug	PBPK model	absorbed × intestinal availability, $F_a F_g$	absorption rate constant, $k_a$ (1/h)	distribution volume, $V_1$ (L)	hepatic intrinsic clearance, $CL_{\text{h, int, in vivo}}$ (L/h)	hepatic clearance, $CL_h$ (L/h)	$AUC_{\text{last}}$ , $\text{ng h}^{-1} \text{mL}^{-1}$
caffeine	human, from humanized mice	1	0.50	18.6	4.91	4.35	26200
	human, average ( $\pm$ SD)	1	0.97 ( $\pm$ 0.57)	58.1 ( $\pm$ 29.4)	7.25 ( $\pm$ 1.71)	4.83 ( $\pm$ 2.52)	16700 ( $\pm$ 6000)
	literature						21,300 ( $\pm$ 9,530)
S-warfarin	human, from humanized mice	1	7.51	5.90	2.54	0.259	17000
	human, average ( $\pm$ SD)	1	2.74 ( $\pm$ 3.03)	9.7 ( $\pm$ 4.4)	2.90 ( $\pm$ 2.41)	0.25 ( $\pm$ 0.26)	13900 ( $\pm$ 3380)
	literature						16,000 ( $\pm$ 4,340)
omeprazole	human, from humanized mice	1	2.84	77.2	2020	52.2	229
	human, average ( $\pm$ SD)	1	2.59 ( $\pm$ 1.84)	37.2 ( $\pm$ 26.9)	1340 ( $\pm$ 513)	40.9 ( $\pm$ 9.9)	407 ( $\pm$ 216)
	literature						368 ( $\pm$ 250)
metoprolol	human, from humanized mice	1	1.65	174	105	46.5	1300
	human, average ( $\pm$ SD)	1	0.91 ( $\pm$ 0.48)	200 ( $\pm$ 66)	178 ( $\pm$ 110)	55.9 ( $\pm$ 10.6)	939 ( $\pm$ 347)
	literature						449 ( $\pm$ 303)
midazolam	Human, from humanized mice	1	2.37	62	475	31.7	53.5
	Human, average ( $\pm$ SD)	1	1.00 ( $\pm$ 0.82)	71 ( $\pm$ 33)	827 ( $\pm$ 352)	41.5 ( $\pm$ 10.4)	37.5 ( $\pm$ 17.4)
	Literature						23.7 ( $\pm$ 8.0)

Estimates of human plasma concentrations of various P450 probes were based on non-human primates, dog, and minipig plasma data.<sup>31–33</sup> Average parameters for humans were calculated with human PBPK models based on five animal models. Values in parentheses are SD values. Literature values<sup>57</sup> are  $\pm$ SD.